



This is the accepted manuscript made available via CHORUS. The article has been published as:

Angular momentum for black hole binaries in numerical relativity

Ritesh Bachhar, Richard H. Price, and Gaurav Khanna

Phys. Rev. D **108**, 064019 — Published 12 September 2023

DOI: [10.1103/PhysRevD.108.064019](https://doi.org/10.1103/PhysRevD.108.064019)

Angular Momentum for Black Hole Binaries in Numerical Relativity

Ritesh Bachhar

Department of Physics, East Hall, University of Rhode Island, Kingston, RI 02881

Richard H. Price

Department of Physics, MIT, 77 Massachusetts Ave., Cambridge, MA 02139

Gaurav Khanna

*Department of Physics and Center for Computational Research,
University of Rhode Island, Kingston, RI 02881 and*

*Department of Physics and Center for Scientific Computing & Data Research,
University of Massachusetts, Dartmouth, MA 02747*

The extensive catalog of waveforms, with details of binary black hole inspiral and merger, offer an opportunity to understand black hole interactions beyond the large separation regime. We envision a research program that focuses on the transfer of angular momentum from spin of the individual holes to the orbital angular momentum and the role of tidal coupling in the process. That analysis will require the formulation of an expression for the orbital angular momentum of a binary, an expression that is useful at small separations, since that regime is well out of the range of Newtonian approximations and is where tidal coupling should be most interesting. We report here such an expression, a binary orbital angular momentum based on numerical relativity results for quasi-circular orbits, that agrees remarkably well with a similar quantity constructed with particle-perturbation techniques for the Kerr geometry.

I. INTRODUCTION

Computational modeling of binary black hole dynamics, once a fantasy, is now so mature that a publicly accessible summary of results for more than two thousand models, i.e., the SXS catalog, [1, 2] is available. These models start at separations large enough that they can be well approximated by a model of two point masses, moving according to Newtonian physics, and losing energy and angular momentum in gravitational wave (GW) emission approximated by the quadrupole formula. This relatively simple approach, and its extensions, have been known as the particle-perturbation method (PP), and were the main tool for understanding binary inspiral until the conquest by numerical relativity (NR) [3] in the early part of the new millennium.

Numerical relativity can do what PP cannot do. Highly developed numerical relativity (NR) codes extend binary black hole evolution from the early PP-appropriate era to the formation and ringdown of the final remnant black hole. In principle, these numerical evolutions give us a laboratory for extracting nonlinear effects through comparisons using PP and with insights and vocabulary based on the PP picture.

Our primary interest in exploiting the NR results is the role of black hole spin. The SXS catalog includes the spins of each of the two initial black holes, and the spin of the single remnant hole. Intuition suggests that negligible angular momentum can be radiated during the plunge following the binary equivalent [4] of the innermost stable circular orbit (ISCO). It is easily verified that the angular momentum in the remnant Kerr hole is well approximated by the binary orbital angular momentum (BOAM) at the plunge [6]. For cases in which the initial

holes have spin, most of that spin angular momentum appears in the Kerr remnant as an addition to the ISCO orbital angular momentum [7].

It is important to note that for the inspiral of holes with initial spins, the role of spin is not simply a storage of angular momentum until the remnant is formed. This can be seen in the effect of the spins on the evolution of the binary. Cases in which there is significant spin aligned in the same direction as the BOAM evolve more slowly than spinless evolution; cases with initial spins anti-aligned, evolve more quickly. We take this as a hint that the angular momentum of the spins is being transferred to the BOAM. In the case of aligned BOAM-spin this transfer increases the BOAM requiring increased time for the GW radiation of the BOAM, and for the inward evolution of the binary. The opposite is the case for initial anti-alignment.

This transfer is what is usually called spin-orbit coupling, and – for ordinary astrophysical bodies – is understood as brought about by tidal torque. That torque is due to the tidal bulge¹ on the torqued body being out of alignment with the line connecting the center of the torqued object and the source of the tidal effects. The root of this misalignment is the viscosity of the material in the torqued object.

Black holes have no “material.” By black hole we typically mean an event horizon, a “teleologically” de-

¹ Here the word “bulge” is meant to be suggestive only. Since the shape of the horizon can be given different meanings, we will not ascribe quantitative meaning to the “bulge,” or to the tidal Love number related to that bulge.

defined mathematical surface, a surface defined by the no-escape condition in the infinite future. How such a non-material entity can have viscosity is therefore of great interest. Work on this question dates back at least to 1973 [9, 11, 12]. That work was chiefly based on the effect of a point particle perturbation on a Kerr hole [13]. More recently, Poisson [14] has compared black hole process and those of fluid bodies. That work should give us at least a very approximate measure of how much angular momentum is transferred via tidal coupling. The results presented here will be a necessary first step in determining whether the angular momentum of the binary remnant is compatible with the limits suggested by those approximations.

In brief, the strategy we will follow is to start with NR data, available from a “hybridized” surrogate model NRHybSur3dq8 [22] trained with NR and Post-Newtonian waveforms. In this paper, we will use that NR data for evolution of a binary with no initial spins. From that NR data we establish a BOAM that is useful in considerations of angular momentum conservation. It is interesting that we find that this NR-based BOAM agrees better than might be expected with BOAM inferred from the PP results for the Kerr geometry.

The NR-based BOAM will be used in a subsequent paper [23] to infer the evolution of the black hole spins from conservation of angular momentum. That spin evolution will then be compared to simple models of tidal torque based on the strength of tidal effects and difference of the orbital velocity of a hole and the angular velocity Ω_H [14] of its event horizon.

The rest of this paper is organized as follows. In Sec. II A we briefly review the SXS data relevant to the role of spin in binary evolution, then in Sec. II B we show how the NR data for GW emission can be used to construct a BOAM that is meaningful for a study of spin-orbit exchange of angular momentum. In Sec. III we present numerical results for the BOAM identified in Sec. II, compare it with the Newtonian approximation, and use a fitting to produce what will be necessary for our study of tidal interaction: the NR-based BOAM as a function of the orbital velocity. Section IV presents our method for adapting, from PP theory, the angular momentum for a point particle orbiting a Kerr hole to a binary of comparable masses. We summarize our conclusions in Sec. V.

Throughout this paper we generally use units in which $c = G = 1$, although factors of G are sometimes explicit. In our plots, all quantities will be normalized by the total system mass M . We will consistently use the symbol L to denote BOAM, while J will mean angular momentum more generally, in particular in connection with GW emission. We will follow the practice of Ref. [1] of using the symbol χ to denote the angular momentum of an individual hole divided by the square of the mass of that hole, and for positive χ to indicate alignment with the BOAM.

We start, in Fig. 1, with a suggestive look at a possi-

ble effect of angular momentum transfer. In that figure we see the phenomenon mentioned above. As compared to the waveform for no initial spins, the one for initial spins aligned with BOAM is slower to reach the end of quasicircular orbiting, and the waveform for the initially anti-aligned spins is faster. As expected, the shifts among waveform phases are dramatic as the end of quasicircular orbiting is approached. What is encouraging about these NR results, however, is that there is significant differences of phase among the three cases, sufficiently early that they can be understood with the approximation methods we will be using.

Although Fig. 1 is an encouraging introduction, the GW waveforms are not the optimal data for understanding the details of black hole interactions. Throughout this paper, and subsequent investigations including spin, our go-to technique will be to look at various kinematic and dynamic quantities as functions of the orbital or gravitational wave angular frequency. It will become clear that this approach often simplifies comparisons, and avoids ambiguities. Note that throughout this paper, time t refers to the Schwarzschild time coordinate, equivalently the time at infinity.

Lastly, it is worth emphasizing that the interactions we are pursuing are of primary importance in the strong field regime. We are, in fact, using NR results to understand the strong field regime. While well-established techniques, like the post-Newtonian (PN) approximations are of great importance for the early evolution of the binary, we do not make use of them here.

II. BACKGROUND: SPIN-ORBIT COUPLING EVIDENCE FROM NR AND OUR APPROACH

A. Evidence from SXS

The ISCO [4] represents a sharp change in the evolution of the binary. Prior to the ISCO the evolution is a slow quasi-adiabatic decrease in the radius of the circular binary orbit [5]. It is in the pre-ISCO motion that GWs carry away energy and angular momentum of the system. The plunge subsequent to the ISCO is rapid, and it is a reasonable assumption that it entails negligible loss of energy or angular momentum.

This suggests [6, 10] that, in the case of holes with no initial spin, the BOAM at the ISCO shows up as the spin of the “remnant” Kerr hole that is the end point of the evolution. Buonanno *et al.* [7] have taken a step further, and have shown that in the case of holes with initial spins, the Kerr remnant spin is well approximated by the vector sum of those spins and the BOAM at the ISCO.

While the appearance of orbital angular momentum in the spin of the remnant hole is intuitively appealing, the mechanism for the contribution of the individual hole spins is less obvious, and hence more interesting. Our working hypothesis is that the individual spins are trans-

ferred to the BOAM during the late pre-ISCO stage of inspiral. Evidence of this can be seen in SXS models with nonzero initial values of the dimensionless parameter χ , the spin angular momentum of a hole divided by the square of the hole's mass. As an example we can compare equal mass models SXS:BBH:0161 and SXS:BBH:0164. In the former, each hole has spin $\chi = -0.3$, where the minus sign indicates anti-alignment of the spins with the BOAM. The latter model, SXS:BBH:0164, differs only in that initially it has aligned spin and BOAM, i.e., $\chi = +0.3$. [8]

We note that for the $\chi = -0.3$ model, the time to the ISCO is approximately 4,250 in units of the total binary mass, while for the $+0.3$ model the time is 5,025. This fits our viewpoint that spin is being transferred to BOAM. For 0161, the $\chi = -0.3$ model, the transfer of angular momentum decreases the BOAM and decreases the time necessary to shed the BOAM as GW emission. The opposite applies to 0164, the $\chi = +0.3$ model.

The details of the GW waveforms, as proxies for the orbital angular motion, offer a somewhat deeper insight. The 0161 waveform phase starts to lead that of 0164 relatively early in the evolution (at time around 2,500) when the separation of the black holes is on the order of 14 in units of the binary mass, a separation at which we might expect relativistic effects to appear but not dominate. At later times, the rate at which the phases of 0161 and 0164 deviate increases, as we would expect in view of the sensitivity of tidal effects to separation (the sixth power of the separation! [13, 14]).

It is important, at this point, to ask whether there is another explanation for what is observed in the comparison of the 0161 and 0164 SXS waveforms. Is there another explanation for the more rapid evolution of the binary with anti-aligned spins than with aligned spins. There are two such possibilities. (1) For a binary with spinning holes, the binary energy and angular momentum are different than if the holes were nonspinning. Thus the time required for shedding energy and angular momentum in GWs would be affected. (2) The rate of GW emission of a binary is affected by the spins of the individual holes in the binary.

The first possibility deserves careful inspection since the ISCO for a point particle around a Kerr hole is different for a prograde and a retrograde orbit. For a Kerr hole with mass M and spin parameter $a = 0.3M$, the prograde/retrograde ISCOs are respectively at radii 4.979 and 6.949 in units of M . One would therefore not be surprised if the equivalent of the ISCO for a *binary* would be smaller, and therefore later, for binaries with aligned spin than for anti-aligned spin. The effect, a manifestation of GR effects in the interaction of the holes, might also be an element in the $\chi = 0.3$ vs -0.3 phase shift noted in the earlier waveforms. This matter will be discussed in some depth in our subsequent paper [23]. For now, we point out that it is a part of the motivation for the exploration of ideas in Sec. IV. The second alternative explanation of observed shifts, the sensitivity of GW emission to spins

of the holes, seems unphysical, since the generation of the GW emission (at least for “particles” moving well below lightspeed) is associated with the distant fields of the sources.

B. A meaningful BOAM

We must ask just what it is that we want for a meaningful BOAM. For our purposes, the total angular momentum (BOAM and spin) is lost to the system only in GW emission. In the case that the individual holes have no spin, we therefore seek a quantity that has this feature.

In the absence of spin effects, the BOAM L that we want will therefore be the quantity that satisfies

$$\frac{dL}{dt} = j^{\text{GW}} \quad (1)$$

where j^{GW} is the rate at which GW carries off angular momentum.

If the approximation is to remain valid that the binary orbit remains nearly circular during inspiral, the angular momentum can safely be assumed to be a function of angular velocity (Ω). Now our useful BOAM must satisfy,

$$\frac{dL}{dt} = \dot{\Omega} \frac{dL}{d\Omega}, \quad (2)$$

where the overdot represents a derivative with respect to time. From Eq. (2), we have that $L(\Omega)$ is to be found from

$$\frac{dL}{d\Omega} = \frac{j^{\text{GW}}}{\dot{\Omega}}, \quad (3)$$

in which all quantities on the right can be directly calculated from NR waveform [24].

III. CHARACTERIZING BINARY ORBITAL ANGULAR MOMENTUM

A. Newtonian form

From Newtonian physics, for masses m_1 and m_2 , at distances r_1 , and r_2 , from the barycenter, the orbital angular momentum is

$$L = L_1 + L_2 = m_1 r_1^2 \Omega + m_2 r_2^2 \Omega = M(GM)^{2/3} \Omega^{-1/3} f(q) \quad (4)$$

where

$$f(q) = \frac{1}{(1+q)(1+1/q)}. \quad (5)$$

Here, and throughout this paper, we will find it interesting to compare PP-based quantities with those from

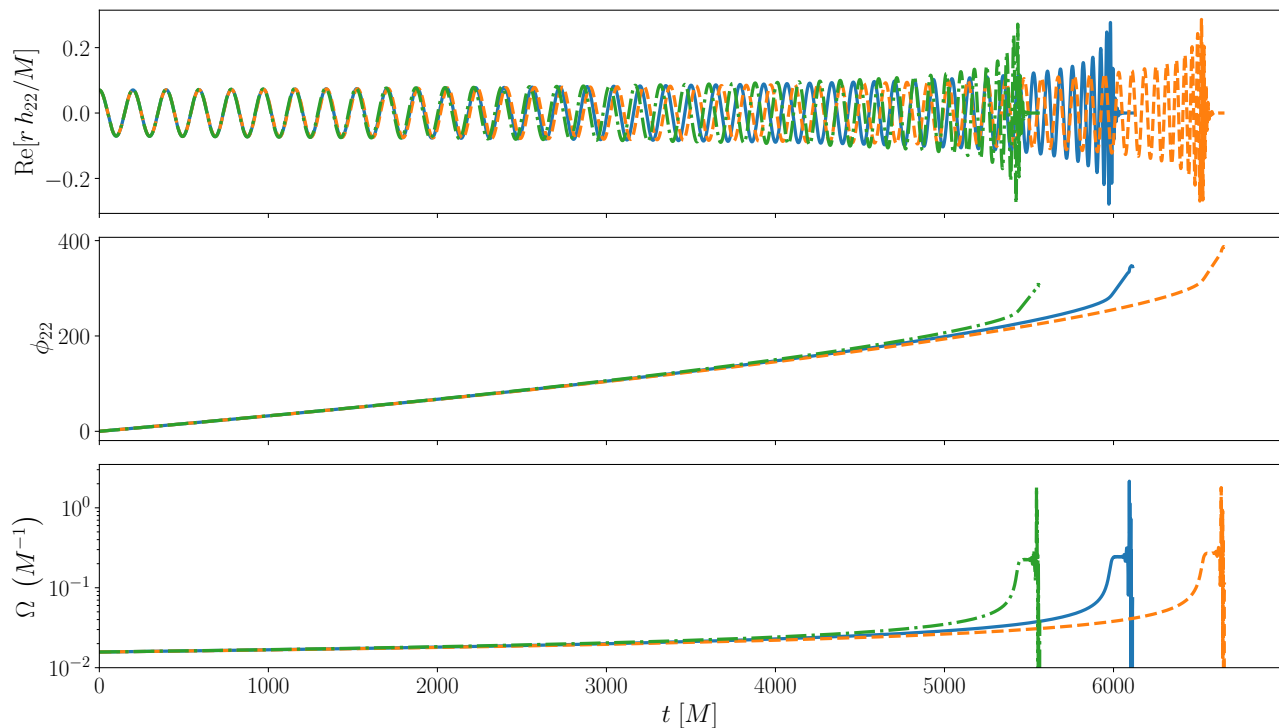


FIG. 1: Real part of (2, 2) waveform (top panel), phase of (2, 2) mode (middle panel), and orbital frequency (bottom panel) as a function of time, for equal mass ratio binaries with no initial spins (blue, solid), with initial spins $\chi = +0.3$ (orange, dashed) for each, and for $\chi = -0.3$ (green, dash-dot) for each. Waveforms are aligned in time such that all three have $\Omega = 0.0157/M$ at the start of evolution. These waveforms correspond to the SXS catalog models BBH:0161 ($\chi = -0.3$), 0001 ($\chi = 0$), and 0164 ($\chi = +0.3$).

NR. From the standard PP result for quadrupole radiation [17] we have

$$\dot{E}^{\text{GW}} = \frac{32}{5} \frac{MG^4 m_1^2 m_2^2}{c^5 r^5} = \frac{32}{5} \frac{M(GM)^4}{c^5 r^5} [f(q)]^2 \quad (6)$$

and the Kepler law

$$\Omega = \sqrt{GM/r^3}, \quad (7)$$

where $r = r_1 + r_2$ is the separation of the point masses. As a function of Ω , the GW energy flux is

$$\dot{E}^{\text{GW}} = \frac{32}{5} \frac{M}{c^5} (GM)^{7/3} \Omega^{10/3} [f(q)]^2. \quad (8)$$

In the Newtonian context, the rate of loss of angular momentum is related to \dot{E}^{GW} , the rate of loss of energy due to GW emission by $\dot{E}^{\text{GW}} = \Omega \dot{J}^{\text{GW}}$. From Eqs. (4), (8) and $dL/dt = \dot{J}^{\text{GW}}$ this gives us

$$\dot{\Omega} = -\frac{96}{5c^5} (GM)^{5/3} \Omega^{11/3} f(q). \quad (9)$$

and hence

$$\frac{\dot{J}^{\text{GW}}}{\dot{\Omega}} = \frac{\dot{E}^{\text{GW}}}{\dot{\Omega}\Omega} = -\frac{1}{3} M(GM)^{2/3} \Omega^{-4/3} f(q). \quad (10)$$

The right-hand side is the Newtonian form we want to compare to the NR results for the left-hand side.

B. Results for numerically inspired BOAM

To obtain the numerical data for the study of binary orbital parameters, we used a “hybridized” NR surrogate model NRHybSur3dq8. This model is trained with Post-Newtonian and EOB waveforms in the early inspiral and smoothly connects to NR data before the merger. Because of this, the model is capable of generating long waveforms, which are ideal for our investigation. We decomposed the complex dominant quadrupole mode ($l = |m| = 2$),

$$h_{22} = A_{22} e^{-i\phi_{22}} \quad (11)$$

into amplitude, A_{22} and phase, ϕ_{22} . The time derivative of the phase (ϕ_{22}) gives us the angular frequency of the signal. Since the binary is a quasi-circular orbit we can calculate the orbital angular velocity (Ω) of the binary using,

$$\omega = \frac{d\phi_{22}}{dt} \quad (12)$$

$$\Omega = \frac{\omega}{2}. \quad (13)$$

Similarly, the time derivative of the orbital angular velocity ($\dot{\Omega}$) can be obtained from

$$\dot{\omega} = \frac{d^2\phi_{22}}{dt^2} \quad (14)$$

$$\dot{\Omega} = \frac{\dot{\omega}}{2}. \quad (15)$$

We adapted the method explained in Ref. [24] to calculate the angular momentum radiated by gravitational waves (j^{GW}). Now we have everything to calculate the left-hand side of Eq. (10). In Fig. 2 we have compared the result obtained from NR data to the Newtonian result. To find a meaningful BOAM for the study of the transfer of angular momentum via tidal coupling, we provide empirical fits for Eq. (3) as a function of orbital frequency, for $q = 1$ and $q = 3$ without spin,

$$\begin{aligned} \left. \frac{dL}{d\Omega} \right|_{q=1} &= - \left(\frac{1}{12} - 0.746\Omega + 2.612\Omega^2 + 13.721\Omega^3 \right) \Omega^{-4/3}, \\ \left. \frac{dL}{d\Omega} \right|_{q=3} &= - \left(\frac{1}{16} - 0.618\Omega + 3.577\Omega^2 - 10.178\Omega^3 \right) \Omega^{-4/3} \end{aligned} \quad (16)$$

The choice of these functions is made such that they converge to Newtonian results in a low orbital frequency limit. $dL/d\Omega$ as a function of Ω is presented in Fig. 2.

IV. KERR-INSPIRED BOAM

Our development of an appropriate expression for the BOAM starts by adapting the particle motion around a Kerr hole as presented, for example, in Refs. [20, 21]. In doing so we are omitting the effect of spin curvature of the smaller body in our calculation, which in fact has negligible effect on the circular equatorial orbit [25]. We present the expressions from Ref. [21] for the conserved angular momentum of a particle of mass μ in a circular orbit of radius r around a Kerr hole of mass M . The meaning of the \pm and \mp signs is related to prograde and retrograde particle motion, and is explained in Ref. [21].

$$\frac{L_{\pm}^{\text{K}}}{\mu} = \frac{\pm M^{1/2} (r^2 \mp 2aM^{1/2}r^{1/2} + a^2)}{r^{3/4} (r^{3/2} - 3Mr^{1/2} \pm 2aM^{1/2})^{1/2}} \quad (17)$$

To treat hole 2 as the ‘‘particle’’ we set $\mu = m_2$, $M = m_1$, $a = \chi_1 m_1$, and take r to be the separation of the holes. Here and below, treating hole 1 as the particle only requires exchanging 1 and 2 on appropriate quantities.

The result of this procedure is *not* what we want since it gives $L_{\text{end}}^{\text{K}}$, the angular velocity about one of the black holes, as a center of rotation. We must adjust this to find the physical angular velocity L_b^{K} , the angular velocity about the barycenter. To do this we multiply $L_{\text{end}}^{\text{K}}$ by the factor that converts $L_{\text{end}}^{\text{K}}$ to L_b^{K} in the Newtonian case. Our notations here: $M = m_1 + m_2$ is the total mass; r_1 and r_2 are distances from the binary’s barycenter to the

individual holes, with $r_1 = r(m_2/M)$, $r_2 = r(m_1/M)$, where r is the distance between them. The reasons behind choosing this approach of calculating BOAM are twofold. First, our method treats each hole on an equal footing, i.e., the spin of each hole is considered in the BOAM calculation. Second, we have discovered in preparation for the following paper [23] that the process mentioned in this section estimates the final BH spin better than other theoretically motivated methods such as [7, 10] over extended parameter space.

Below, we use ‘‘end’’ to refer to dynamical quantities based on one of the holes (m_1 or m_2) as stationary inertial points and ‘‘b’’ as quantities calculated with the barycenter as the stationary inertial point.

We find that the Newtonian angular momentum referred to the two different centers are

$$L_{e1} = m_1 \sqrt{Gm_2} r^{1/2} \text{ and } L_{b1} = m_1 \sqrt{Gm_2} r_1^{3/2} r^{-1}. \quad (18)$$

For the Newtonian expressions then, the conversion from the end value to the barycenter value for hole 1 is

$$\Gamma_1 \equiv \frac{L_{b1}}{L_{e1}} = (1+q)^{-3/2}. \quad (19)$$

The analogous multiplier for particle 2 follows by substituting $1/q$ for q .

We now use Eq. (17) to find the Kerr-inspired angular momentum of hole 1 about hole 2, then convert it to the angular momentum about the barycenter using the same conversion factor Γ_1 , as in Eq. (19). The same procedure is used for the motion of hole 2.

Finally, with L_1^{end} and L_2^{end} from Eq. (17), for appropriate choices of radii and masses, we take the BOAM, $L_{\text{bin}}^{\text{K}}$, to be $\Gamma_1 L_1^{\text{end}} + \Gamma_2 L_2^{\text{end}}$. The result is

$$\begin{aligned} L_{\text{bin}}^{\text{K}} &= \frac{\sqrt{GM}rM}{(1+q)(1+1/q)} \\ &\times \left[\frac{1}{\sqrt{(1+q)(1+q-\frac{3M}{r})}} + \frac{1}{\sqrt{(1+q^{-1})(1+q^{-1}-\frac{3M}{r})}} \right] \end{aligned} \quad (20)$$

when both black holes don’t have spin. The Newtonian equivalent differs only in the absence of the $3M/r$ subtractions inside the square roots. The results in Tables I–III show that the Kerr-inspired values differ significantly from the Newtonian values only when the separation is small and one would expect significant general relativistic effects.

What is most important to the purpose of this paper is to compare these Kerr-inspired results for the BOAM with a measure of the BOAM that has meaning for conservation. This is the NR content of the right-hand side of Eq. (3) in which the meaningful BOAM is taken to be the quantity that is decreased by the angular momentum in outgoing GWs.

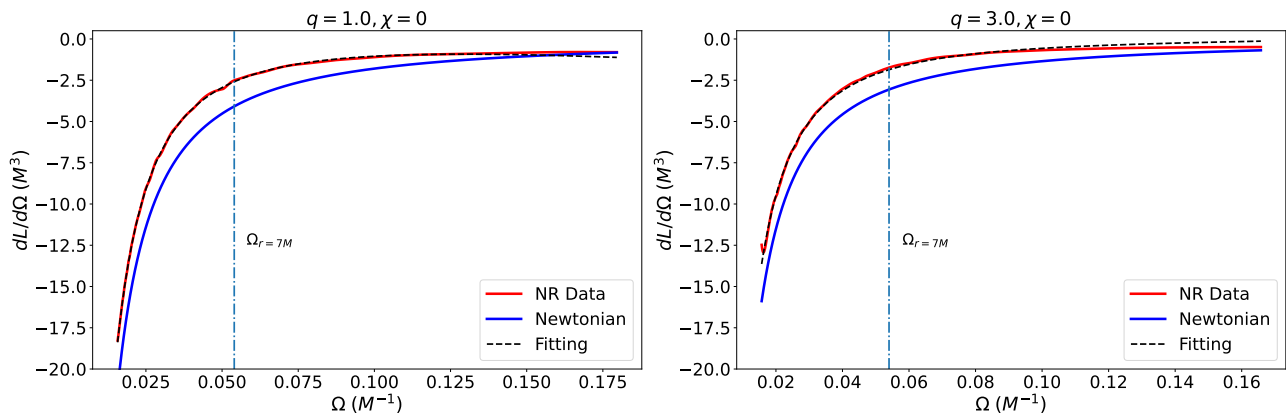


FIG. 2: $dL/d\Omega$ as a function of angular velocity Ω for $q = 1, 3$ with no initial spin. NR data is compared with the Newtonian form and a simple fit is provided. The vertical line corresponds to $dL/d\Omega$ at angular velocity $\Omega = \sqrt{GM/r^3}$ for $r = 7M$, which approximately coincides with the ISCO. The dashed curves show the NR-based fitting given by Eqs. (16).

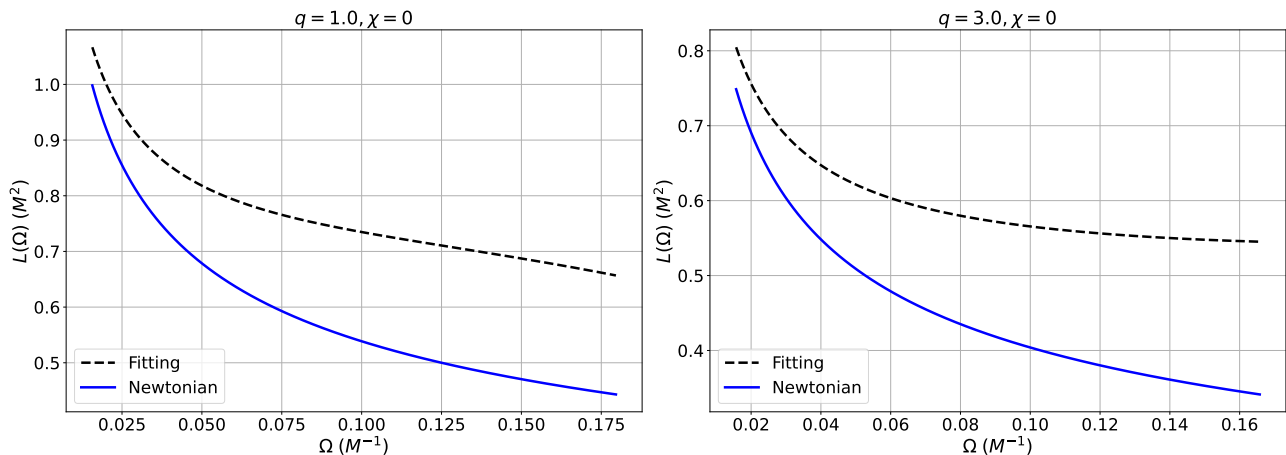


FIG. 3: Angular momentum (L) as a function of angular velocity (Ω) for mass ratio $q = 1$ (left) and $q = 3$ (right) with no initial spin. The Newtonian angular momentum is represented as the blue solid line, while the black dashed line depicts Eqs. (21) for $q = 1$, and (22) for $q = 3$. The Newtonian, and fitting curves asymptotically approach the same values as Ω becomes small.

Integrating the fits given in Eq. (16), we arrive at the expressions,

$$L_{\text{bin}}^{\text{GW}} \Big|_{q=1} = \left(\frac{1}{4} + 1.119\Omega - 1.567\Omega^2 - 5.145\Omega^3 \right) \Omega^{-1/3} \quad (21)$$

$$L_{\text{bin}}^{\text{GW}} \Big|_{q=3} = \left(\frac{3}{16} + 0.926\Omega - 2.146\Omega^2 + 3.817\Omega^3 \right) \Omega^{-1/3} \quad (22)$$

The angular momentum, denoted here as $L_{\text{bin}}^{\text{GW}}$, is presented in Fig. 3 for $q = 1$, and $q = 3$.

Comparisons are given in Table I. In that table, the reasonably good agreement of $L_{\text{bin}}^{\text{GW}}$ and $L_{\text{bin}}^{\text{K}}$, as r decreases, is an important result. It leads to two important conclusions. First, it adds confidence in our GW-based BOAM, the BOAM that can be used as a conserved quantity in the analysis of angular momentum exchange. Second, as r decreases and GR effects become important,

it agrees better with $L_{\text{bin}}^{\text{K}}$ than with $L_{\text{bin}}^{\text{N}}$. The same fact can also be observed in Fig. 4. This result for binaries without black hole spin adds confidence in applying our approach to adapting Kerr PP results to comparable mass binaries with spin. In Table II and Fig. 5 we have presented our method for spinning cases.

V. CONCLUSIONS

We have provided an important element needed for a NR-based analysis of the transfer of spin to orbital angular momentum, and its connection to black hole tidal coupling: orbital angular momentum that is meaningful for conservation of total angular momentum. This quantity is constructed by formulating a kinematic binary expression related to the rate of emission of gravitational wave angular momentum in the absence of spin. We have found that this NR-based binary angular mo-

TABLE I: Binary angular momentum L_{bin} , in units of the square of the total mass, computed by the approach given in the text, as a function of the binary separation r in units of the total binary mass, for black holes with no initial spin. Values are given for $L_{\text{bin}}^{\text{K}}$, the Kerr-based result given in Eq. (17), for $L_{\text{bin}}^{\text{N}}$ the Newtonian value, and for $L_{\text{bin}}^{\text{GW}}$, the angular momentum inferred from the NR data for emitted angular momentum. Results are given for $q \equiv m_1/m_2 = 1$ and 3. The transition from quasi-adiabatic inspiral to plunge – the binary equivalent of the ISCO, inferred from waveforms – is somewhat less than separation of around $7M$.

r	$L_{\text{bin}}^{\text{K},q=1}$	$L_{\text{bin}}^{\text{N},q=1}$	$L_{\text{bin}}^{\text{GW},q=1}$	$L_{\text{bin}}^{\text{K},q=3}$	$L_{\text{bin}}^{\text{N},q=3}$	$L_{\text{bin}}^{\text{GW},q=3}$
100	2.5190	2.5000	2.5112	1.8928	1.8750	1.8842
50	1.7949	1.7678	1.7901	1.3515	1.3258	1.3442
20	1.1625	1.118	1.1731	0.8812	0.8385	0.8836
10	0.8575	0.7905	0.8970	0.6593	0.5929	0.6791
7	0.7462	0.6614	0.8070	0.5829	0.4961	0.6134

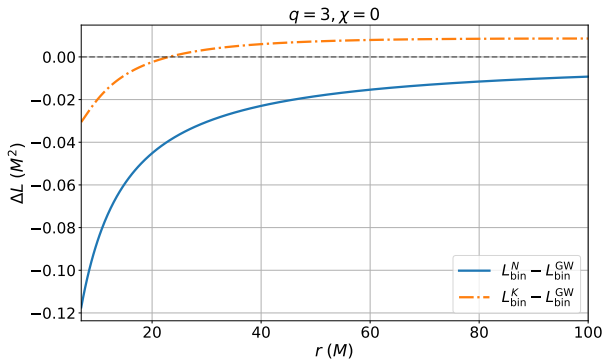


FIG. 4: The cyan line represents the difference between radiated GW angular momentum flux ($L_{\text{bin}}^{\text{GW}}$) and the Newtonian angular momentum $L_{\text{bin}}^{\text{N}}$, for $q = 3$ and $\chi = 0$. The difference between $L_{\text{bin}}^{\text{K}}$, the Kerr-inspired results, and $L_{\text{bin}}^{\text{GW}}$, is depicted in the orange line. The dashed black line is included in the plot to serve as a reference.

mentum differs significantly from Newtonian binary angular momentum at small separation, but is in remarkably good agreement with a binary angular momentum inferred from a particle perturbation treatment rooted in the Kerr geometry.²

The success of our approach to a binary angular momentum is a reason for some confidence that the related approach for angular velocity is more accurate than the Newtonian Kepler law at the small separations at which

² In calculations performed subsequent to the original submission of this paper we used our BOAM prescription and looked at the change in angular momentum from the initial configuration to the ISCO, and compared it to the radiated angular momentum during that time. The agreement was very good, adding confidence in the method of Sec. IV.

TABLE II: Binary angular momentum $L_{\text{bin}}^{\text{K},q=1}$, in units of the square of the total mass, computed by the approach outlined in the text, as a function of the binary separation r in units of the total binary mass, for black holes of equal mass ($q = 1$) and equal values of BH spin χ .

r	$\chi = 0$	$\chi = +0.3$	$\chi = -0.3$	$\chi = +0.5$	$\chi = -0.5$
100	2.5190	2.5182	2.5198	2.5176	2.5203
50	1.7949	1.7933	1.7965	1.7922	1.7976
20	1.1625	1.1583	1.1668	1.1556	1.1697
10	0.8575	0.8486	0.8669	0.8429	0.8733
7	0.7462	0.7327	0.7607	0.7242	0.7708

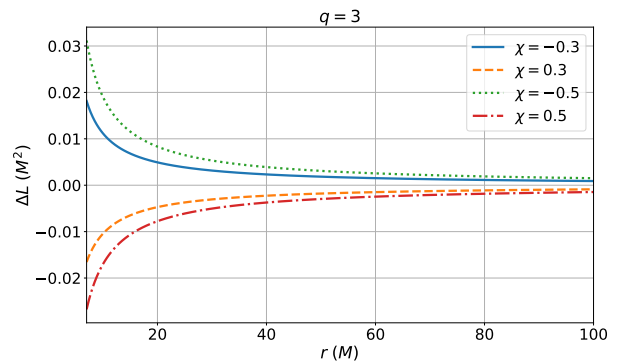


FIG. 5: This plot depicts the deviation of $L_{\text{bin}}^{\text{K},q=3}$ for $\chi \neq 0$ from $L_{\text{bin}}^{\text{K},q=3}$ for $\chi = 0$ case as the binary approaches ISCO.

tidal transfer is significant.

The elements provided in this paper will be used in the formulation of a paper [23] on tidal torque inferred from the waveforms in the SXS catalog.

Acknowledgments: R.B and G.K. acknowledge support from NSF Grants No. PHY-2106755 and No. DMS-1912716. All computations were performed on the UMass-URI UNITY HPC/AI cluster at the Massachusetts Green High-Performance Computing Center (MGHPCC).

TABLE III: Binary angular momentum $L_{\text{bin}}^{K,q=3}$, in units of the square of the total mass, computed by the approach outlined in the text, as a function of the binary separation r in units of the total binary mass, for black holes with mass ratio 3:1 ($q = 3$) and equal values of BH spin χ .

r	$\chi = 0$	$\chi = +0.3$	$\chi = -0.3$	$\chi = +0.5$	$\chi = -0.5$
100	1.8928	1.8920	1.8938	1.8914	1.8944
50	1.3515	1.3497	1.3533	1.3485	1.3546
20	0.8812	0.8765	0.8862	0.8735	0.8896
10	0.6593	0.6488	0.6704	0.6422	0.6783
7	0.5829	0.5664	0.6011	0.5562	0.6141

-
- [1] Michael Boyle *et al.*, *Class. Quant. Grav.* **36**, 195006 (2019); Abdul Mroue *et al.* *Phys. Rev. Lett.* **111**, 241104 (2013).
- [2] SXS Collaboration, SXS Waveform Catalog <https://data.black-holes.org/waveforms/catalog.html>
- [3] Thomas W. Baumgarte and Stuart L. Shapiro, *Numerical Relativity: Solving Einstein's Equations on the Computer*, Cambridge University Press <https://doi.org/10.1017/CB09781139193344> (2010).
- [4] For a radiating binary of comparable masses there is no conserved mechanical energy, so no “ISCO” in the PP sense. For simplicity, we shall continue to use the term ISCO to mean the onset of the plunge. The actual time of the plunge can be well approximated from the SXS waveforms.
- [5] P. C. Peters, *Phys. Rev.* **136**, B1224 (1964).
- [6] Scott A. Hughes, Robert D. Blandford, *Astrophys. J.* **585**, L101 (2003).
- [7] Alessandra Buonanno, Larry E. Kidder, and Luis Lehner, *Phys. Rev. D* **77** 026004 (2008).
- [8] The “initial” parameters of a model are the data fed into the initial solver. The SXS catalog also provides parameters at a “reference” time, after the early “junk” radiation has dissipated. For models 0161 and 0164, the differences are less than 10%.
- [9] James B. Hartle, *Phys. Rev. D* **8**, 1010 (1972).
- [10] Richard H. Price and Gaurav Khanna, *Phys. Rev. D* **106**, 084037 (2022).
- [11] James B. Hartle, *Phys. Rev. D* **9**, 2749 (1973).
- [12] Richard H. Price, John T. Whelan, *Phys. Rev. Lett.* **87**, 231101 (2001).
- [13] Eric Poisson, *Phys. Rev. D* **70**, 084044 (2004).
- [14] Eric Poisson, *Phys. Rev. D* **80**, 064029 (2009).
- [15] A. E. H. Love, *Proc. R. Soc. Lond. A* **82** (1909).
- [16] A. E. H. Love, *Some problems of geodynamics*, Cornell University Library, Ithaca (1911).
- [17] P. C. Peters and J. Mathews, *Phys. Rev.* **131**, 435 (1963). The relevant result is quoted as Charles W. Misner, Kip S. Thorne, and John A. Wheeler, *Gravitation* (W. H. Freeman, San Francisco, 1973) Eq. 36.16a.
- [18] Charles W. Misner, Kip S. Thorne, and John A. Wheeler, *Gravitation* (W. H. Freeman, San Francisco, 1973) Eq. 33.2.
- [19] Daniela Pugliese, Hernando Quevedo and Remo Ruffini, *Phys. Rev. D* **84**, 044030 (2011).
- [20] D. Bini, R. T. Jantzen, *Class. Quantum Grav.* **17**, 16371647 (2000).
- [21] James M. Bardeen, William H. Press, Saul A Teukolsky, *The Astrophysical Journal* **178** (1972).
- [22] Vijay Varma, Scott E. Field, Mark A. Scheel, Jonathan Blackman, Lawrence E. Kidder, Harald P. Pfeiffer, *Phys. Rev. D* **99**, 064045 (2019).
- [23] Richard Price and Ritesh Bacchar, *in preparation*.
- [24] Davide Gerosa, François Hébert, Leo C. Stein, *Phys. Rev. D* **97**, 104049 (2018).
- [25] Drummond, Lisa V. and Hughes, Scott A., *Phys. Rev. D* **105**, 124041 (2022).